metals

MDPI

Article

Advanced Mechanical Strength in Post Heat Treated SLM 2507 at Room and High Temperature Promoted by Hard/Ductile Sigma Precipitates

Kamran Saeidi [1], Sajid Alvi [1], Frantisek Lofaj [2], Valeri Ivanov Petkov [1] and Farid Akhtar [1,*]

[1] Division of Materials Science, Department of Engineering Sciences and Mathematics, Luleå University of Technology, SE-97187 Luleå, Sweden; kamran.saeidi@ltu.se (K.S.); sajid.alvi@ltu.se (S.A.); ivapet-2@student.ltu.se (V.I.P.)

[2] Department of Ceramics, Institute of Mater. Res. of the Slovak Academy of Sciences, Watsonova 47, 04001 Košice, Slovakia; flofaj@saske.sk

* Correspondence: farid.akhtar@ltu.se; Tel.: +46-706-209-750

Received: 21 January 2019; Accepted: 31 January 2019; Published: 8 February 2019

Abstract: Duplex stainless steel, 71 wt.% austenite, 13 wt.% ferrite and 16 wt.% sigma, was made upon heat treating of fully ferritic as-built selective laser melted (SLM) 2507 stainless steel at 1200 °C. Formation of sigma phase in the heat treated SLM 2507 was investigated using optical microscopy and scanning electron microscopy (SEM). The heat treated SLM 2507 demonstrated a yield strength of 686 MPa, ultimate tensile strength of 920 MPa and an elongation of 1.8% at room temperature with a brittle fracture morphology. Precipitation of sigma phase during heat treatment and slow cooling improved the mechanical and wear properties at high temperatures (1200 °C and 800 °C, respectively). The tensile strength and elongation of the heat treated SLM 2507 was measured 400 MPa and 20% as compared to casted duplex steel with 19 MPa and 30% elongation at 1200 °C. The 20 times higher mechanical strength as compared to casted duplex steel was attributed to sigma precipitates. Tribological behaviour of heat treated duplex SLM 2507 containing sigma at 800 °C showed very low wear rate of 4.5×10^{-5} mm^3/mN compared to casted duplex steel with 1.6×10^{-4} mm^3/mN.

Keywords: selective laser melting; duplex stainless steel; heat treatment; mechanical properties

1. Introduction

The Additive manufacturing (AM) has emerged as a flexible technique to manufacture components with intricate geometries and enhanced properties [1]. Amongst AM techniques, selective laser melting (SLM) fabricates near fully dense metallic materials and alloys using high energy laser source to melt and bond metal/alloy powder particles layer by layer [2]. High temperature, asymmetric thermal gradients and fast cooling rates are characteristic of SLM and result in evolution of unique microstructures and superior properties of sintered materials [3]. Numerous metallic materials including titanium alloys [4,5], aluminium alloys [6], nickel-based superalloys [7], stainless steels [8–10] have been fabricated using SLM. Regarding SLM processing of steels, most of the efforts have been devoted to austenitic 316L, maraging steel and Inconel [11–13] with a few studies by Saeidi et al. [9] and Davidson et al. [14] on the microstructure evolution and mechanical properties of duplex stainless steels.

Duplex stainless steels (DSS) have an approximately equal phase balance of ferrite and austenite in the microstructure. The chemical composition and thermal history of the steel influences the phase balance of ferrite and austenite in DSS. DSS offer a favourable combination of properties rendering these steels suitable for oil and gas, steam boilers, reaction vessels, petrochemical, pulp and paper, pollution control and marine industries [15–17]. Continuous developments of duplex stainless steels

have led to steel compositions with substantial amount of alloying elements. Addition of alloying elements influences the composition, microstructure and can improve mechanical properties [18]. One limitation of using DSS is the numerous phase transformations occurring in broad temperature range from 300 °C to 1300 °C [19,20]. The intermetallic phases precipitate and induce a negative effect on the toughness and performance of DSS [21,22]. The commonly found intermetallic phases in stainless steels are sigma, Khi and Laves phases. As a rule, the intermetallic phases are enriched with chromium and molybdenum as compared to the nominal composition. Therefore, precipitation of intermetallic phases is normally associated with undesirable depletion of alloying elements, such as chromium and molybdenum [23], from the matrix. In contrast, precipitation of Sigma phase can induce a strengthening effect in DSS where the sigma precipitates nucleating at grain boundaries act as barriers against dislocation movement and make the material strong. Davanageri et al. [24] reported that precipitation of sigma phase improved the mechanical strength and the wear resistance of the material.

Rapid cooling of steels from high temperatures can influence the Cr_{eq}/Ni_{eq} and effect the phase transformations. Saeidi et al. [9] observed suppression of austenite in 2507 duplex stainless steel during SLM process and reported formation of fully ferritic material. Recent work by Hengbach et al. [25] reported the effect of heat treatment and quenching on fully ferritic SLM 2205 duplex stainless steel where heat treatments at 900 °C, 1100 °C and 1200 °C of the duplex SLM were carried out and the fraction of austenite and ferrite phases were determined using EBSD technique at each temperature and room temperature mechanical properties of the heat treated SLM duplex steels were reported. It was found that at none of the heat treatment temperatures sigma had been precipitated, the fraction of austenite was the highest at 1100 °C and mechanical properties were the highest for the SLM duplex steel heat treated at 1200 °C. The mechanical performance of the heat-treated specimens was determined and compared with each other. Despite the work conducted by Hengbach et al. [25] using SLM, the effect of post heat treatment on SLM duplex stainless steel and the effect of cooling rate on precipitation of intermetallic phase and its influence on the microstructure evolution has not been studied and co-related to room and high temperature mechanical properties.

The formation of sigma phase and its effect on microstructure and mechanical properties and wear behaviour at room and high service temperature (for example, in boilers) in SLM manufactured duplex stainless steel has not been studied and is of attention for industries. Thus, in this research work, formation of intermetallic sigma precipitates in the microstructure of duplex stainless steel via heat treatment of SLM 2507 is reported and the effect of heat treatment and precipitation of intermetallic sigma phase on materials chemistry, microstructure evolution, mechanical strength and sliding wear at room and high service temperature are studied and compared with the conventional casted duplex steel.

2. Materials and Methods

Nitrogen-gas atomized Duplex SAF2507 stainless steel powder (supplied by Sandvik Osprey Ltd., Neath, UK) with particle size of 32–45 μm was used as starting material. The overall chemical composition of the as-received powder provided by the manufacturer is 25% Cr, 7% Ni, 4% Mo, 0.8% Si, 0.3% N, 1.2% Mn, <0.03% C (all in wt.%).

The specimens for tensile testing and wear test were generated using an EOS M270 selective laser melting (SLM) device, supplied by EOS group (EOS, Krailing, Germany), equipped with a 200 W ytterbium fibre laser. For data preparation, the software Magics (Version 7, Materialise, Bremen, Germany) was utilized. Via SLM, tensile bars (10 mm length × 10 mm width × 80 mm height) were manufactured and for wear test cubic samples (30 mm length × 30 mm width × 2 mm thickness) were manufactured. Laser processing parameters used were 200 W power, 0.1 mm line spacing, 750 mm/s scan speed with a layer thickness of 20 micron.

The heat treatment process was carried out on the SLM bars in a tubular furnace in Ar atmosphere where the samples were heated to 1200 °C and soaked for 5 min and cooled down in furnace with a cooling rate $\geq$ 300 °C/h.

For microstructure observation the heat treated SLM bars were cut into smaller pieces and mechanically ground, polished and electro etched in 20 mol. % NaOH solution at 3 V for 10 s. Optical microscopy was performed with a Nikon optical microscope (ECLIPSE MA200, Tokyo, Japan). Detailed microstructure characterization by scanning electron microscopy (SEM)/Energy-dispersive X-ray spectroscopy (EDS) was carried out using a JEOL SEM (JSM-IT300LV, Tokyo, Japan). X-Ray Diffraction data, of the heat-treated sample was collected using a PANalytical X'Pert Pro diffractometer with a copper radiation source (40 mV voltage and 20 mA current) in 2θ range of 40°–100°. Reitveld refinement was used for phase quantification. To prepare a sample for EBSD analysis, the heat-treated sample was electro-polished carried out on a Struers (Lectro Pol-5, Hovedstaden, Ballerup, Denmark) at 30 V for 15 s. The EBSD analysis was performed using a JSM-IT300LV equipped with Oxford NordlysMax (JEOL Inc., Peabody, MA, USA).

The tensile tests were performed at room temperature and high temperature 1200 °C using two different test setup and equipment. Room temperature tensile test was carried out on SLM duplex bars heat treated at 1200 °C and furnace cooled with dimension of 40 mm × 4 mm × 1 mm using a universal testing machine TiraTest 2300 (Tira GmbH, Schalkau, Germany) with the force head of 100 kN. The crosshead speed was 0.1 mm/min was used. High temperature (1200 °C) tensile test was done by Gleeble 3800 thermo-mechanical simulator (Dynamic Systems Inc., Poestenkill, NY, USA) where the SLM bar was heated to 1200 °C and at the same temperature tensile test was carried out. Microhardness measurements were carried out using a MXT-Microhardness tester (MATSUZAWA, SEIKI, Japan). Ten indentations were made, and the average was reported.

High temperature dry sliding was carried out at 800 °C in air atmosphere using ball-on-disc set up in Rtec universal tribometer (Rtec Instruments, San Jose, CA, USA). SLM duplex stainless-steel samples heat treated at 1200 °C were cut into specimens of 30 mm length × 30 mm width × 2 mm thickness and mirror polished, followed by cleaning with acetone using ultrasonicator and drying in an oven at 80 °C before the wear test. Non-porous Al_2O_3 ball with a diameter of 9.5 mm was used as counter surface against heat treated SLM duplex samples, corresponding to maximum Hertzian stress of 937 MPa. A constant load of 10 N, sliding speed of 0.03 m/s and a sliding distance of 200 m was maintained for studying friction and wear behaviour of SLM duplex stainless steel. Wear rate was measured by calculating the ratio of wear volume (mm^3) to sliding distance (m) and normal load (N). In order to calculate wear volume, the samples were cleaned with acetone in an ultrasonic bath and dried in oven at 80 °C, followed by using optical profilometer (Wyko 1100 3D, Bruker Nano Inc., Billerica, MA, USA) to get an average depth of wear from 16 different points in the wear track.

3. Results

The relative density, determined by Archimedes method, of heat treated SLM 2507 was 99% of theoretical density, suggesting near full dense material. The room temperature (RT) tensile behaviour of heat treated SLM 2507 is shown in Figure 1a and the corresponding mechanical properties are summarized in Table 1. The specimen has a yield strength of 686 MPa (according to the linear elastic part of the curve), tensile strength of 920 MPa (according to the plateau of the curve) and an elongation of 1.8% before failure. The measured relative density of the heat treated SLM 250 (99%) suggests that the low elongation of 1.8% is not only due to the flaws in the material but also due to the presence of intermetallic phases rich in Cr and Mo; sigma phase [24]. As seen from Table 1, the tensile strength of the heat treated SLM 2507 is higher than as-casted and solution treated duplex stainless steel [26] and heat treated SLM duplex 2205 material [25]. Fracture surface micrographs in Figure 1b,c shows cleavage fracture without any sign of ductile fracture. Figure 1c shows phases enriched in Cr and Mo which are shown by energy dispersive spectroscopy (EDS) data taken from the three points with corresponding Cr and Mo values in Figure 1d. The Mo and Cr contents, 6.5–9.3 wt.% Mo and

31.3–31.8 wt.%, are significantly higher than the starting powder, which contains 4 wt.% Mo and 25 wt.% Cr. This confirms that the brittle behaviour of SLM 2507 is correlated to the presence of phases enriched in Mo and Cr.

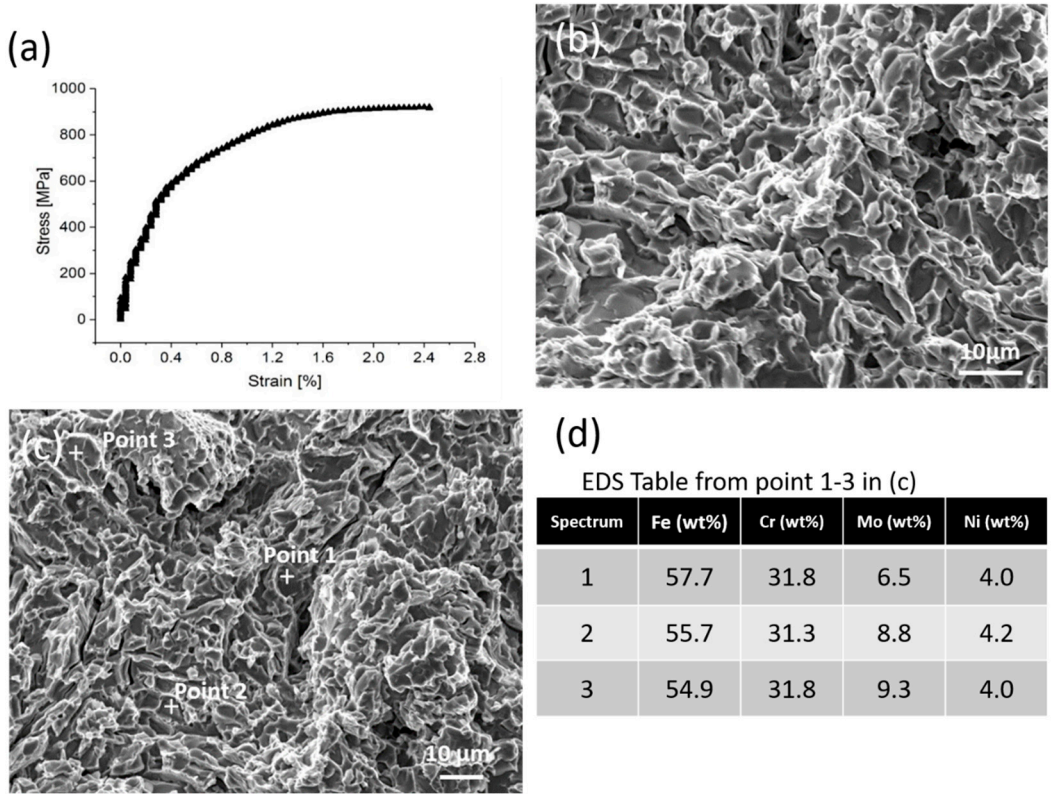

Spectrum	Fe (wt%)	Cr (wt%)	Mo (wt%)	Ni (wt%)
1	57.7	31.8	6.5	4.0
2	55.7	31.3	8.8	4.2
3	54.9	31.8	9.3	4.0

Figure 1. (**a**) Room temperature tensile test curve of post heat treated SLM 2507. (**b**,**c**) Fractography at different magnifications taken from the sample and Energy-dispersive X-ray spectroscopy (EDS) taken from (**c**) where the percentage of Cr and Mo representing the presence of intermetallic sigma phase is shown in EDS data Table in (**d**).

Table 1. Room temperature mechanical properties of selective laser melted (SLM) duplex post heat treated at 1200 °C and as-built SLM and as-casted duplex stainless steel.

Material	Tensile Strength (MPa)	Elongation (%)	Microhardness (Hv)
Post heat treated SLM 2507 (this work)	920 MPa	1.8%	400 Hv
As built-SLM 2507 [9]	1320 MPa	8%	450 Hv
Post heat treated SLM 2205 [25]	750 MPa	20%	-
Heat treated conventional duplex [26]	649 MPa	34%	227 Hv
As Casted duplex [26]	660 MPa	29%	235 Hv

The microhardness of the heat treated SLM 2507 was around 400 Hv, which is twice as high as casted duplex material [26] and comparable with as-built SLM 2507 duplex material reported earlier [9]. Considering the fact that the heat treatment relieves the residual stresses of as-built SLM 2507, the high microhardness is possibly due to the presence of hard phase such as sigma/Khi phases in the material (which is not present in as-built SLM 2507). Hsieh et al. [27] has reported higher hardness of stainless steels due to the presence of sigma phase.

X-ray diffraction (XRD) phase analysis of as-built SLM 2507 and the heat treated SLM 2507 is shown in Figure 2a,b respectively. The as-built SLM 2507 contains ferrite. And, the heat treated SLM 2507 shows that ferrite has partially transformed to austenite with austenite content of 71 wt.% and ferrite measured 13 wt.%, determined by Reitveld refinement of XRD data. Furthermore, secondary phases, sigma and Khi, are identified. The sigma and Khi phase quantification is approximated to

16 wt.% by Reitveld refinement (with R_{exp} = 2.1) with majority being sigma phase. The underlying mechanism for the precipitation formation has been discussed and explained in literature in detail and therefore it will not be further discussed in this work. It can be assumed that the high strength and low plasticity (1.8% elongation) is caused by the presence of relatively high amount of intermetallic sigma phase. Therefore, despite having high amount of austenite (71 wt.% austenite, Figure 2a), the plasticity of the heat treated SLM 2507 steel is low and therefore it fails in brittle mode (Figure 1). Earlier it has been reported [21] that in intermetallic phases the metal atoms have defined positions in the crystal lattice reducing the number of available slip planes for dislocation movements. This creates very high stacking fault energies (SFE) which is higher than the bond energies holding the atoms together, causing brittleness [21]. Low plasticity (lower than 4%) was reported by Kim et al. [28], where the mechanical behaviour of duplex stainless steel containing sigma precipitates were studied. Hau et al. [29] investigated the sigma phase embrittlement and reported that the presence of sigma phase in stainless steel resulted in loss of ductility and toughness at room temperature. Ezuber et al. [30] reported that ductility and toughness of the material was reduced significantly with even small volume fraction of sigma phase. Furthermore, Martins et al. [31] showed that the loss of ductility would increase with increasing sigma concentration. The percentage of intermetallic phases (majority being sigma phase) formed in the heat treated material in current work is 16 wt.% which is considerably large. Therefore, the formation of intermetallic sigma phase has resulted in low plasticity of the material (1.8% elongation).

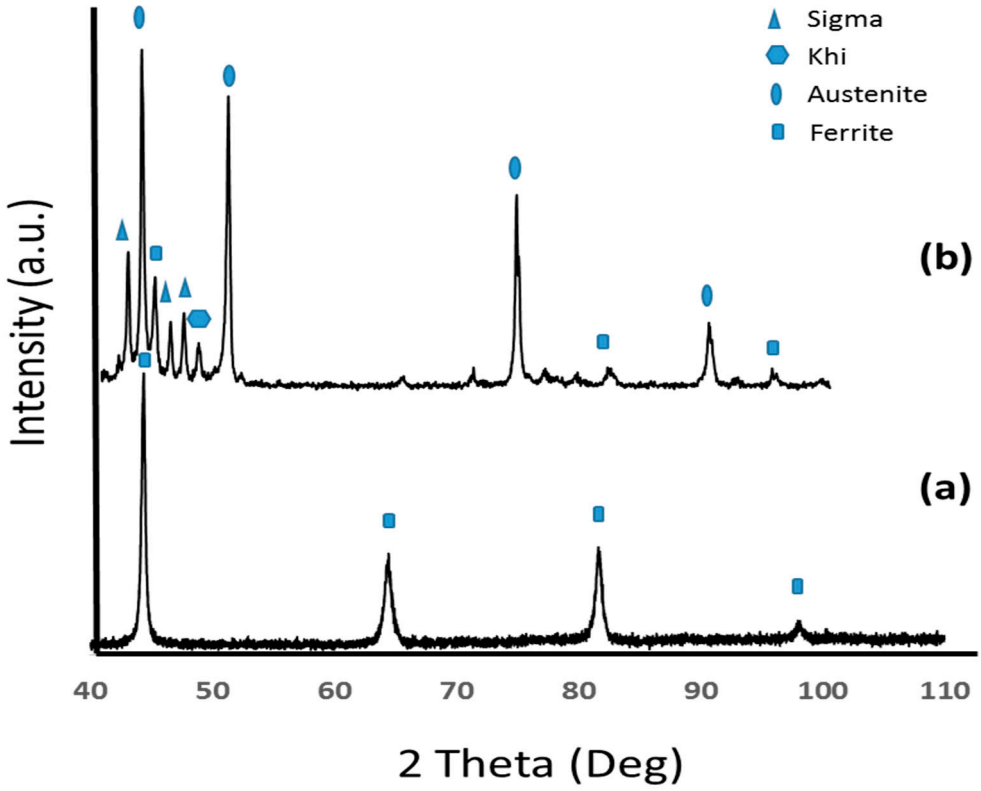

Figure 2. X-ray diffraction (XRD) phase analysis of SLM DSS 2507; (**a**) and as-built, (**b**) heat treated at 1200 °C.

Optical microscopy images of the heat treated SLM 2507 in Figure 3a show a mosaic type macro texture (designed by the scanning strategy during SLM) with tesserae around 100 µm. Inside the tesserae, widmanstäten austenite and columnar austenite were observed, as shown by the red dashed circle and arrows in Figure 3b,c and ferrite phase is seen in between the austenitic grains (according to as-built SLM 2507, the ferrite phase is the parent phase and austenite nucleates and grows after).

The columnar austenitic grains are restricted by the tesserae boundaries and controlled by them with size less than 100 µm and width around 5–10 µm, while the widmanstäten austenite are much smaller around 10–40 µm length (Figure 3c). In between the tesserae, secondary austenite grains are formed with random morphology and size ranging from 3–5 µm.

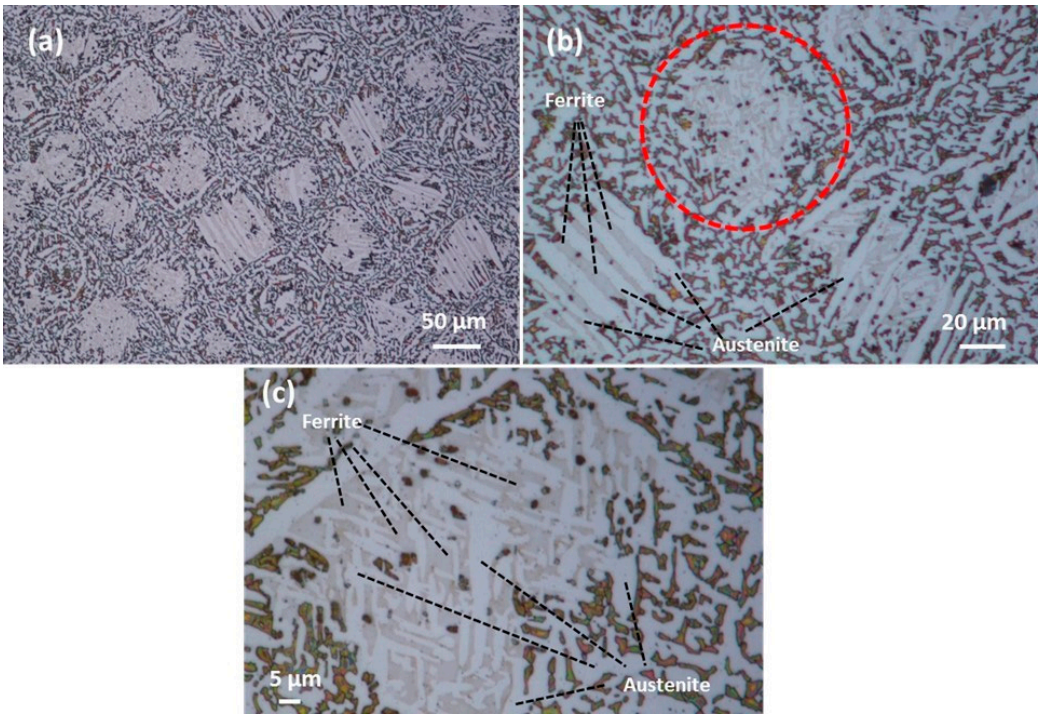

Figure 3. Optical imaging of the heat treated sample (**a**) mosaic texture containing austenite and ferrite grains (**b**) columnar austenite grains and ferrite grains in between austenite (**c**) higher magnification of the circled part in (**b**) showing Widmanstäten-like austenite grains and ferrite grains in between.

Figure 4 illustrates detailed microstructure of the post heat treated SLM 2507. As labelled by arrows in Figure 4b, apart from austenite and ferrite, sigma and Khi phases are observed with dark and black contrast, respectively. Intermetallic sigma and Khi phases have been observed by electron microscopy observations and reported by others [32,33]. Figure 4 demonstrates that the sigma phase is large in content which is in good agreement with the phase quantification using XRD data.

The high temperature tensile test at 1200 °C of heat treated SLM 2507 is shown in Figure 5a. From the tensile curve it is seen that the material strains until it reaches a plateau of 50 MPa and undergo 7% luders strain. Further, strain is accompanied with strain strengthening leading to withstanding stresses up to 400 MPa which upon this stage, the material deforms until failure. The tensile test curve was repeatable in all the test. The mechanical properties are listed in Table 2 and compared with high temperature mechanical properties of conventional casted duplex steel. As seen the tensile strength of the heat treated SLM 2507 with 400 MPa is 20 times higher than the strength of conventional casted duplex of 19 MPa [34]. It is assumed that the very high mechanical strength is due to both; the sigma precipitates and the fine microstructure observed in Figures 3 and 4. To establish the effect of sigma precipitates, as-built SLM 2507 was heat treated at 1200 °C and cooled down rapidly to avoid formation of sigma precipitates. Thereafter, the mechanical strength of the post heat treated SLM 2507 (without any sigma precipitates) obtained at 1200 °C was measured approximately 200 MPa with total elongation of 30% before failure (Table 2). Therefore, it was deduced that the mechanical strength of 400 MPa is due to combination of the formation of sigma precipitates along with the fine microstructure of SLM alloy. It has been mentioned in the literature [35] that sigma phase is disappeared at temperature around 900 °C, thus, to clarify the existence of sigma phase at high

temperature, in-situ high temperature XRD was performed on the heat treated sample at 1000 °C (highest applicable test temperature for in-situ XRD equipment), the results showed existence of sigma along with austenite and ferrite phases as seen in Figure 6. The heat treated SLM 2507 containing sigma phase showed ductility of 20% (Table 2) compared to 1.8% elongation at room temperature. This has been previously observed by Levin et al. [36] where it was claimed that sigma phase was plastic at high temperature tensile tests and the material's plasticity was improved. Fracture surface of the heat treated SLM 2507 sample in Figure 5b confirms that the specimen fails in a dual ductile-brittle mode with small sized dimples (seen in Figure 5b) and sigma precipitates that are enriched in Cr and Mo shown by the point EDS taken from Figure 5c with corresponding Cr and Mo values reported in Figure 5d.

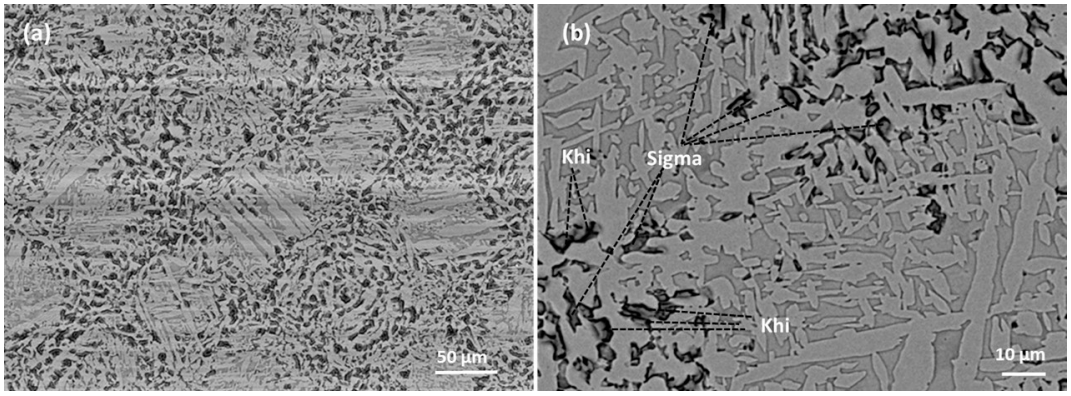

Figure 4. (**a**,**b**) Back scattered SEM image showing existence of austenite, ferrite and intermetallic sigma and Khi phases. Sigma and Khi phases are shown with arrows in (**b**).

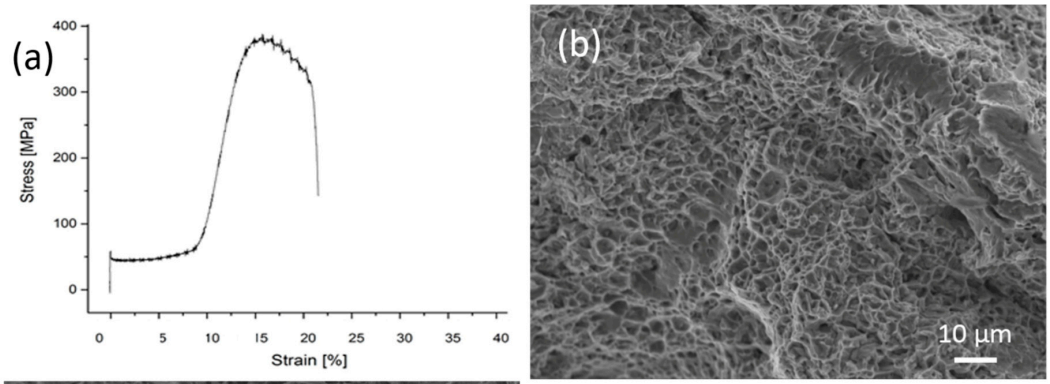

(d)

EDS table for point 1-5 in (c)

Spectrum	Fe (wt%)	Cr (wt%)	Mo (wt%)	Ni (wt%)
1	57.2	31.4	6.5	4.8
2	56.9	31.8	6.4	4.8
3	56.8.	32.2	6.6	4.4
4	56.1	33.3	6.9	3.7
5	58.0	31.8	5.8	4.5

Figure 5. (**a**) Tensile test curve of post heat treated SLM 2507 obtained at 1200 °C, (**b**,**c**) Fracture analysis of the Showing overall dimples and cleavages, EDS taken from (**c**) where the percentage of Cr and Mo representing sigma is shown in EDS data Table in (**d**).

Table 2. High temperature mechanical properties of post heat treated SLM 2507 obtained at 1200 °C and comparison with conventional casted duplex steel at the same temperature.

Tensile Test at 1200 °C	Tensile Strength (MPa)	Elongation (%)
Post heat treated SLM 2507 (this work)	400 MPa	20%
As-built SLM duplex (this work)	200 MPa	30%
Conventional duplex [34]	19 MPa	-

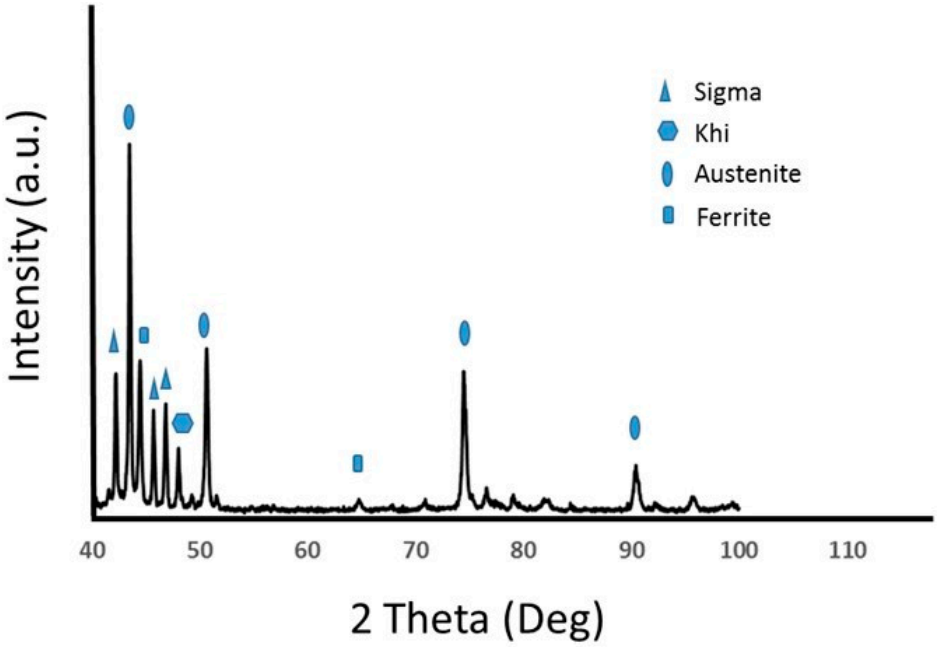

Figure 6. In-situ high temperature XRD phase analysis of SLM DSS 2507 taken at 1000 °C showing existence of ferrite, austenite and intermetallic sigma phase.

Friction and wear of post heat treated SLM 2507 at 800 °C was studied against Al_2O_3 ball (shown in Figure 7 and Table 3). The test showed a steady coefficient of friction (COF) of 0.65, after initial run-in period, for a sliding distance of 200 m, as shown in Figure 7a. The profiles of wear track showed an average depth of 8.8 µm and a wear rate of 4.5 × 10^{-5} mm^3/N.m, as shown in Figure 7b and Table 3, respectively. Furthermore, the formation of high amount of iron oxide in the wear track, as shown in Figure 7c, acted as a third body lubricant or glazing and hindered wear. The SEM images of wear track in Figure 7c and corresponding higher magnification image in the inset clearly shows less abrasive wear due to the presence of hard sigma phases and formation of film formed by shearing of worn debris. The formation of thin and tough oxide layer has been reported to be due to lower sliding speed [24], which in our case was 0.03 m/s. Previous work by Rotundo et al. [37], showed the discontinuity of iron oxide protective layer in the wear track after wear tests at 300 °C in 316L stainless steel. In contrast, the backscattered image of the wear track, at 800 °C in present work, in Figure 7d and corresponding elemental mapping from the marked region, clearly shows the uniform distribution of iron oxide resulting from oxidation, compaction and sintering of wear debris. The formation of grooves in the sliding direction from local stress by asperity contact led to abrasive wear through ploughing and followed by formation of oxide at the surface. Previous work by Stott et al. [38], has shown that generation of oxide debris is favoured at high temperature leading to compaction of wear debris to form wear protective layers. Furthermore, wear through ploughing mechanism can be explained due to the presence of high amount of hard sigma phases [39].

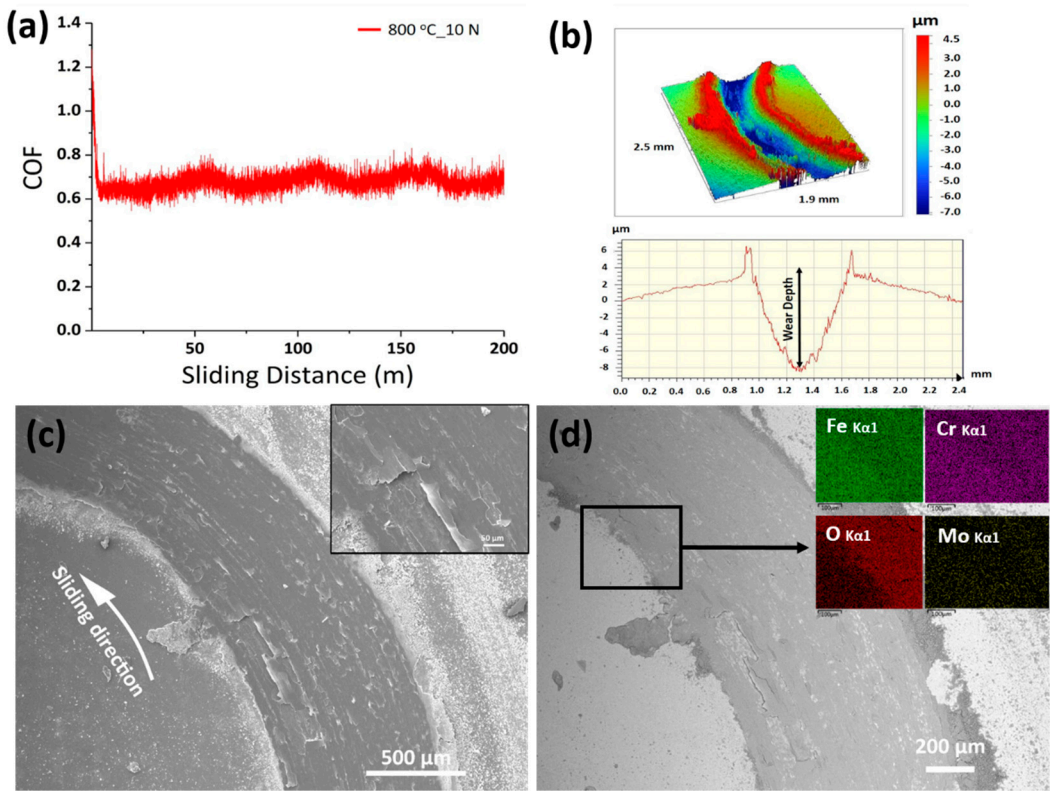

Figure 7. Friction and wear behaviour of post heat treated SLM 2507: (**a**) coefficient of friction (COF) versus sliding distance, (**b**) 3D view of wear track and 2D wear track profile showing wear depth; SEM images of wear track using (**c**) secondary electron mode and (**d**) backscattered electron mode.

Table 3. Sliding wear properties of post heat treated SLM 2507 versus conventional post heat treated DSS.

Material	Wear Volume (mm^3)	Wear Rate (mm^3/mN)	Ave. COF
SLM DSS (800 °C, 10 N load) (This work)	0.003819	4.5×10^{-5}	0.6
Heat treated DSS (RT, 20 N load) [39]	0.8–1	$2–2.5 \times 10^{-4}$	0.4
Heat treated DSS 2507 (RT, 30 N load) [40]	0.01	1.66×10^{-6}	-
Plasma Nitrided F53 DSS (RT, 8–16 N load) [41]	0.25–0.5	$1.25–1.75 \times 10^{-4}$	-

4. Conclusions

In conclusion, heat treatment at 1200 °C of as-built SLM 2507 with fully ferritic phase results in formation of dual austenite and ferrite phases. The fine microstructure and large concentration of Sigma precipitates made the material much stronger than casted duplex steel but very brittle at room temperature with (1.8% elongation). Sigma phase precipitates resulted in high mechanical strength (400 MPa compared to 19 MPa in casted duplex steel), much higher ductility (20% as compared to 1.8%) and very low wear rate (4.5×10^{-5} mm^3/mN compared to casted duplex steel) when exposed to high temperature tensile test (at 1200 °C) and tribology (at 800 °C). Therefore, heat treatment of duplex stainless steel can tailor the high temperature mechanical properties and wear behaviour of duplex stainless steel significantly expanding its application and service temperature.

Author Contributions: K.S. devised all the manuscript except the tribology section, performed all the mechanical testing, XRD analysis and microstructure analysis; S.A. performed the tribology work and wrote the section on tribology; F.L. performed the room temperature mechanical testing of heat treated 2507 duplex sample; V.I.P. performed the sample metallography and prepared the samples; F.A. is the main supervisor and reviewed the whole text and modified it.

Funding: This research was funded by Carl Tryggers foundation (grant No. CTS 16:6) and Swedish Foundation for Strategic Research (SSF) for infrastructure fellowship grant (RIF14-0083) for current research.

Acknowledgments: The authors would like to thank the technical support from the materials lab at Luleå University of Technology.

Conflicts of Interest: The authors declare no conflict of interests.

References

1. Berman, B. 3-D printing: The new industrial revolution. *Bus. Horiz.* **2012**, *55*, 155–162. [CrossRef]
2. Shifeng, W.; Shuai, L.; Qingsong, W.; Yan, C.; Sheng, Z.; Yusheng, S. Effect of molten pool boundaries on the mechanical properties of selective laser melting parts. *J. Mater. Process. Technol.* **2014**, *214*, 2660–2667. [CrossRef]
3. Saeidi, K. Stainless steels fabricated by laser melting: Scaled-down structural hierarchies and microstructural heterogeneities. Ph.D. Thesis, Department of Materials and Environmental Chemistry (MMK), Stockholm University, Stockholm, Sweden, 19 May 2016.
4. Leuders, S.; Thöne, M.; Riemer, A.; Niendorf, T.; Tröster, T.; Richard, H.; Maier, H. On the mechanical behaviour of titanium alloy TiAl6V4 manufactured by selective laser melting: Fatigue resistance and crack growth performance. *Int. J. Fatigue* **2013**, *48*, 300–307. [CrossRef]
5. Song, B.; Dong, S.; Zhang, B.; Liao, H.; Coddet, C. Effects of processing parameters on microstructure and mechanical property of selective laser melted Ti6Al4V. *Mater. Des.* **2012**, *35*, 120–125. [CrossRef]
6. Rao, H.; Giet, S.; Yang, K.; Wu, X.; Davies, C.H. The influence of processing parameters on aluminium alloy A357 manufactured by Selective Laser Melting. *Mater. Des.* **2016**, *109*, 334–346. [CrossRef]
7. Tillmann, W.; Schaak, C.; Nellesen, J.; Schaper, M.; Aydinöz, M.; Hoyer, K.-P. Hot isostatic pressing of IN718 components manufactured by selective laser melting. *Addit. Manuf.* **2017**, *13*, 93–102. [CrossRef]
8. Saeidi, K.; Gao, X.; Zhong, Y.; Shen, Z.J. Hardened austenite steel with columnar sub-grain structure formed by laser melting. *Mater. Sci. Eng. A* **2015**, *625*, 221–229. [CrossRef]
9. Saeidi, K.; Kevetkova, L.; Lofaj, F.; Shen, Z. Novel ferritic stainless steel formed by laser melting from duplex stainless steel powder with advanced mechanical properties and high ductility. *Mater. Sci. Eng. A* **2016**, *665*, 59–65. [CrossRef]
10. Krakhmalev, P.; Yadroitsava, I.; Fredriksson, G.; Yadroitsev, I. In situ heat treatment in selective laser melted martensitic AISI 420 stainless steels. *Mater. Des.* **2015**, *87*, 380–385. [CrossRef]
11. Wang, Y.M.; Voisin, T.; McKeown, J.T.; Ye, J.; Calta, N.P.; Li, Z.; Zeng, Z.; Zhang, Y.; Chen, W.; Roehling, T.T. Additively manufactured hierarchical stainless steels with high strength and ductility. *Nat. Mater.* **2018**, *17*, 63–71. [CrossRef]
12. Fortunato, A.; Lulaj, A.; Melkote, S.; Liverani, E.; Ascari, A.; Umbrello, D. Milling of maraging steel components produced by selective laser melting. *Int. J. Adv. Manuf. Technol.* **2018**, *94*, 1895–1902. [CrossRef]
13. Kanagarajah, P.; Brenne, F.; Niendorf, T.; Maier, H. Inconel 939 processed by selective laser melting: Effect of microstructure and temperature on the mechanical properties under static and cyclic loading. *Mater. Sci. Eng. A* **2013**, *588*, 188–195. [CrossRef]
14. Davidson, K.; Singamneni, S. Selective laser melting of duplex stainless steel powders: An investigation. *Mater. Manuf. Processes* **2016**, *31*, 1543–1555. [CrossRef]
15. Adhe, K.; Kain, V.; Madangopal, K.; Gadiyar, H. Influence of sigma-phase formation on the localized corrosion behaviour of a duplex stainless steel. *J. Mater. Eng. Perform.* **1996**, *5*, 500–506. [CrossRef]
16. Chen, T.; Yang, J. Effects of solution treatment and continuous cooling on σ-phase precipitation in a 2205 duplex stainless steel. *Mater. Sci. Eng. A* **2001**, *311*, 28–41. [CrossRef]
17. Femenia, M.; Pan, J.; Leygraf, C.; Luukkonen, P. In situ study of selective dissolution of duplex stainless steel 2205 by electrochemical scanning tunnelling microscopy. *Corros. Sci.* **2001**, *43*, 1939–1951. [CrossRef]
18. Plaut, R.L.; Herrera, C.; Escriba, D.M.; Rios, P.R.; Padilha, A.F. A short review on wrought austenitic stainless steels at high temperatures: Processing, microstructure, properties and performance. *Mater. Res.* **2007**, *10*, 453–460. [CrossRef]
19. Padilha, A.F.; Aguiar, D.; Plaut, R. Duplex Stainless Steels: A Dozen of Significant Phase Transformations. *Defect Diffus. Forum* **2012**, *322*, 163–174. [CrossRef]
20. Totten, G.E. *Steel Heat Treatment Handbook, -2 Volume Set*; CRC Press: Boca Raton, FL, USA, 2006.
21. Reick, W.; Pohl, M.; Padilha, A. Three Types of Embrittlement in Ferritic-Austenitic Duplex Stainless Steels. *Metal. Int.* **1990**, *3*, 46–50.

22. Calliari, I.; Straffelini, G.; Ramous, E. Investigation of secondary phase effect on 2205 DSS fracture toughness. *Mater. Sci. Technol.* **2010**, *26*, 81–86. [CrossRef]
23. AF, P. Decomposition of austenite in austenitic stainless steels. *ISIJ Int.* **2002**, *42*, 325–327.
24. Davanageri, M.B.; Narendranath, S.; Kadoli, R. Effect of Sigma (σ) phase on Mechanical and Dry sliding wear. *Mater. Today Proc.* **2017**, *4*, 10189–10196. [CrossRef]
25. Hengsbach, F.; Koppa, P.; Duschik, K.; Holzweissig, M.J.; Burns, M.; Nellesen, J.; Tillmann, W.; Tröster, T.; Hoyer, K.-P.; Schaper, M. Duplex stainless steel fabricated by selective laser melting-Microstructural and mechanical properties. *Mater. Des.* **2017**, *133*, 136–142. [CrossRef]
26. Ghosh, S.; Mondal, S. Effect of heat treatment on microstructure and mechanical properties of duplex stainless steel. *Trans. Indian Inst. Met.* **2008**, *61*, 33–37. [CrossRef]
27. Hsieh, C.-C.; Wu, W. Overview of Intermetallic Sigma Phase (σ) Precipitation in Stainless Steels. *ISRN Metall.* **2012**, *2012*. [CrossRef]
28. Kim, S.-K.; Kang, K.-Y.; Kim, M.-S.; Lee, J.-M. Low-temperature mechanical behaviour of super duplex stainless steel with sigma precipitation. *Metals* **2015**, *5*, 1732–1745. [CrossRef]
29. Hau, J.L.; Seijas, A.L. Sigma phase embrittlement of stainless steel in FCC service. In Proceedings of the 61st Annual Conference and Exposition (Corrosion 2006), San Diego, CA, USA, 12–16 March 2006. paper no: 06578.
30. Ezuber, H.M.; El-Houd, A.; El-Shawesh, F. Effects of sigma phase precipitation on seawater pitting of duplex stainless steel. *Desalination* **2007**, *207*, 268–275. [CrossRef]
31. Martins, M.; Casteletti, L.C. Effect of heat treatment on the mechanical properties of ASTM A 890 Gr6A super duplex stainless steel. *J. ASTM Int.* **2005**, *2*, 1–14.
32. Cho, H.-S.; Lee, K. Effect of cold working and isothermal aging on the precipitation of sigma phase in 2205 duplex stainless steel. *Mater. Charact.* **2013**, *75*, 29–34. [CrossRef]
33. Llorca-Isern, N.; López-Luque, H.; López-Jiménez, I.; Biezma, M.V. Identification of sigma and chi phases in duplex stainless steels. *Mater. Charact.* **2016**, *112*, 20–29. [CrossRef]
34. Tehovnik, F.; Zuzek, B.; Burja, J. Hot tensile testing of SAF 2205 duplex stainless steel. *Mater. Technol.* **2016**, *50*, 989–993.
35. Elmer, J.; Palmer, T.; Specht, E. In-situ observation of sigma phase dissolution in 2205 duplex stainless steel using synchtron X-ray diffraction. *Mater. Sci. Eng. A* **2006**, *459*, 151–155. [CrossRef]
36. Levin, E.; Pivnik, E.; Libman, P. The effect of sigma phase on the mechanical properties of heat resistant steels. *Met. Sci. Heat Treat.* **1959**, *1*, 19–21. [CrossRef]
37. Rotundo, F.; Ceschini, L.; Martini, C.; Montanari, R.; Varone, A. High temperature tribological behaviour and microstructural modifications of the low-temperature carburized AISI 316L austenitic stainless steel. *Surf. Coat. Technol.* **2014**, *258*, 772–781. [CrossRef]
38. Stott, F. High-temperature sliding wear of metals. *Tribol. Int.* **2002**, *35*, 489–495. [CrossRef]
39. Fargas, G.; Mestra, A.; Mateo, A. Effect of sigma phase on the wear behaviour of a super duplex stainless steel. *Wear* **2013**, *303*, 584–590. [CrossRef]
40. Davanageri, M.B.; Narendranath, S.; Kadoli, R. Influence of Heat Treatment on Microstructure, Hardness and Wear Behavior of Super Duplex Stainless Steel AISI 2507. *Am. J. Mater. Sci.* **2015**, *5*, 48–52.
41. Pereira Neto, J.O.; Silva, R.O.d.; Silva, E.H.d.; Moreto, J.A.; Bandeira, R.M.; Manfrinato, M.D.; Rossino, L.S. Wear and Corrosion Study of Plasma Nitriding F53 Super duplex Stainless Steel. *Mater. Res.* **2016**, *19*, 1241–1252. [CrossRef]